Research Article

Journal of PeptideScience

Received: 5 April 2011 Revised: 31 May 2011 Accepted: 3 June 2011 Published online in Wiley Online Library: 1 August 2011

(wileyonlinelibrary.com) DOI 10.1002/psc.1390

The conformational properties of α,β-dehydroamino acids with a *C*-terminal ester group

Dawid Siodłak,* Justyna Grondys and Małgorzata A. Broda

α,β-Dehydroamino acid esters occur in nature. To investigate their conformational properties, a systematic theoretical analysis was performed on the model molecules Ac-ΔXaa-OMe [ΔXaa = ΔAla, (*E*)-ΔAbu, (*Z*)-ΔAbu, ΔVal] at the B3LYP/6-311++G(d,p) level in the gas phase as well as in chloroform and water solutions with the self-consistent reaction field-polarisable continuum model method. The Fourier transform IR spectra in CCl_4 and $CHCl_3$ have been analysed as well as the analogous solid state conformations drawn from The Cambridge Structural Database. The ΔAla residue has a considerable tendency to adopt planar conformations C5 ($\phi, \psi \approx -180^\circ, 180^\circ$) and $\beta 2$ ($\phi, \psi \approx -180^\circ, 0^\circ$), regardless of the environment. The ΔVal residue prefers the conformation $\beta 2$ ($\phi, \psi \approx -120^\circ, 0^\circ$) in a low polar environment, but the conformations α ($\phi, \psi \approx -55^\circ, 35^\circ$) and β ($\phi, \psi \approx -55^\circ, 145^\circ$) when the polarity increases. The ΔAbu residues reveal intermediate properties, but their conformational dispositions depend on configuration of the side chain of residue: (*E*)-ΔAbu is similar to ΔAla, whereas (*Z*)-ΔAbu to ΔVal. Results indicate that the low-energy conformation $\beta 2$ is the characteristic feature of dehydroamino acid esters. The studied molecules constitute conformational patterns for dehydroamino acid esters with various side chain substituents in either or both *Z* and *E* positions. Copyright © 2011 European Peptide Society and John Wiley & Sons, Ltd.

Keywords: conformational analysis; dehydroamino acids; depsipeptides; DFT calculations; FTIR spectra; phomalide

Introduction

α,β-Dehydroamino acids with a *C*-terminal ester linkage are present in naturally occurring peptides. Dehydroalanine methyl ester is present in siomycins and thiopeptins, highly modified sulfur-containing macrocyclic peptides. These thiopeptide antibiotics largely inhibit the growth of Gram-positive bacteria [1]. Dehydroalanine with a thioester group is present in antitumor cyclic depsipeptide BE22179 [2]. (*Z*)-Dehydrotyrosine with *C*-terminal ester bond was found in bicyclodecadepsipeptide antibiotic dityromycin [3]. All these peptides are produced by bacteria of the genus *Streptomyces*. Cyrmenins, isolated from myxobacteria strains *Archangium gephyra* and *Cystobacter armeniaca* are *N*-acyldipeptides containing 3-O-methyl-(*Z*)-dehydroserine methyl ester. They reveal promising antifungal activity and exhibit an exceptionally low toxicity for animal cell cultures [4]. An interesting example is phomalide, a selective phytotoxin produced by the fungus *Leptosphaeria maculans*, responsible for leaf spot and stem cankers (blackleg), one of the most damaging diseases of oilseed Brassicas, particularly canola [5–10]. Phomalide is a cyclic pentadepsipeptide containing an unusual (*E*)-dehydrobutyrine residue with *C*-terminal ester linkage (Figure 1). Interestingly, isophomalide containing (*Z*)-dehydrobutyrine residue reveals no activity, whereas the saturated analogue, dihydrophomalide, causes chlorotic lesions on brown mustard but not on canola [9,10]. These results indicate that not only the presence of the dehydroamino acid residue but also its proper geometric isomer is crucial for selective phytotoxicity. Although, there is no data-concerning conformations adopted by the molecules of phomalide and isophomalide, the example rises the problem of the conformational properties of the *Z*/*E* isomers of α,β-dehydroamino acids and an influence they would have on conformations of constituted molecules. Dehydrobutyrine is the simplest dehydroamino acid which reveals the isomerisation *Z*/*E* of the side chain, and thus it is convenient residue to investigate this phenomenon. Additionally, the introduction of an ester instead of amide group within α,β-dehydroamino acid residue can potentially create a new structural unit having specific properties that have not been studied so far. In this article, we report on the first studies of the conformational properties of α,β-dehydroamino acids esters.

Experimental Methods

Theoretical Calculation

The conformational properties of α,β-dehydroamino acids were studied on the basis of the following molecules of *N*-acetyl-α,β-dehydroamino acid methyl esters: Ac-ΔAla-OMe, Ac-(*E*)-ΔAbu-OMe, Ac-(*Z*)-ΔAbu-OMe, and Ac-ΔVal-OMe (Figure 2) using the Gaussian 09 package [11]. Calculations were performed on the *trans*-amide bonds ($\omega_0, \omega_1 \sim 180^\circ$). The ϕ, ψ potential energy surfaces of the studied molecules were created on the basis of 84 points calculated at the B3LYP/6-311++G** level of theory. In each of these structures, the geometrical parameters were fully relaxed, except for the constrained torsion angles ϕ and ψ. The 30° increment was applied for the ϕ, ψ main chain dihedral angles, within the range -180° to 150° for the torsion angles ϕ and within

* *Correspondence to: Dawid Siodłak, Faculty of Chemistry, Opole University, Oleska 48, 45-052 Opole, Poland. E-mail: dsiodlak@uni.opole.pl*

Faculty of Chemistry, Opole University, Oleska 48, 45-052 Opole, Poland

Journal of PeptideScience

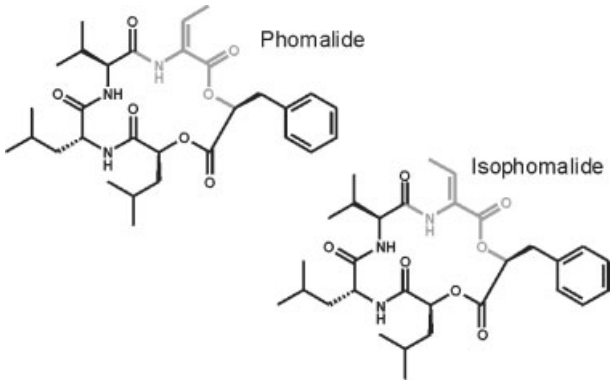

Figure 1. The structure of naturally occurring phomalide and izophomalide-containing dehydrobutyrine with an ester group.

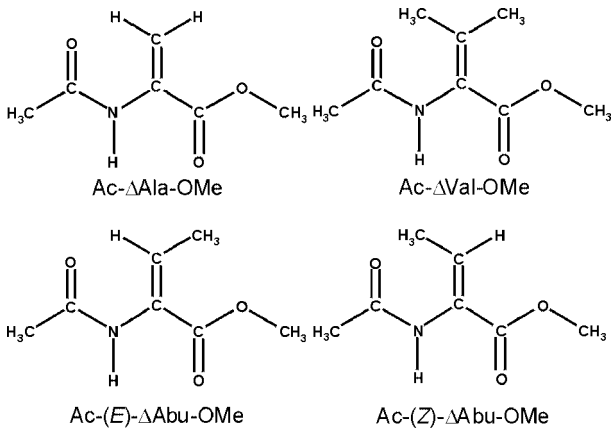

Figure 2. General formula of the model compounds containing the residues studied in this work.

the range 0°–180° for the torsion angles ψ. Due to the achiral α-carbon, inversion through the centre of symmetry (ϕ, ψ = 0°, 0°) yields equivalent structures [i.e. (ϕ, ψ) → ($-\phi$, $-\psi$)]; therefore full (ϕ, ψ) potential energy surface maps were able to be obtained in this way. The energy surfaces were obtained using the Surfer 8 program with the radial basis function as a gridding method (Golden Software, Inc. 2002, Golden, Colorado, USA). To estimate the effects of environment (chloroform and water) on the shapes of the energy surfaces, the calculations were conducted in each grid point using a self-consistent reaction field model, with the geometrical parameters fully relaxed, except for the constrained torsion angles ϕ and ψ. The polarisable continuum model (PCM) was chosen [12,13]. The possible energy minima of every low-energy region of the potential energy surfaces were checked by full geometry optimisation of the selected structures at the B3LYP/6-311++G** level *in vacuo* as well as in the chloroform- and water-mimicking environment using the PCM model. Frequency analyses were carried out to verify the nature of the minimum state of all the stationary points obtained and to calculate the zero-point vibrational energies.

The notations applied in literature for conformations were invented for standard amino acids. None fits dehydroamino acids, which usually adopt the values of the main chain torsion angles ϕ and ψ close to borderline of the conformational regions of standard analogues. Therefore, some conformers have not been labelled strictly according to the nomenclature to avoid confusion. Three common nomenclatures for diamide models were applied in the tables [14] in order to provide better understanding and for the convenience of the readers.

Synthesis

Ac-(*Z*)-ΔAbu-OMe, Ac-(*E*)-ΔAbu-OMe, and Ac-ΔVal-OMe were obtained according to the Schöllkopf and Meyer method [15]. Ac-ΔAla-OH was obtained according to Ref. 16. The reaction progress was monitored and the homogeneity of products roughly checked on silica gel plates (Kieselgel 60 F254, Merck, Darmstadt, Germany). Melting points were determined by differential scanning calorimetry (DSC 2010, TA Instruments, New Castle, Delaware, USA). HPLC was performed on a Beckman 'System Gold' chromatograph.

Ac-ΔVal-OMe

Purified by crystallisation from ethyl acetate. Crystal was obtained by the slow evaporation of diethyl ether at a low temperature (~5 °C). Purity 100% (HPLC). Melting point 85.84 °C. ^{1}H NMR δ6.70 (1H, s), 3.75 (3H, s), 2.17 (3H, s), 2.09 (3H, s), 1.85 (3H, s); ^{13}C NMR δ168.9 (s), 165.3 (s), 146.4 (s), 121.0 (s), 51.8 (s), 23.1 (s), 22.7 (s), 21.34 (s).

Ac-ΔAbu-OMe

The isomers *Z* and *E* were separated using flash column chromatography using diethyl ether as the eluent. Ac-(*Z*)-ΔAbu-OMe: 100% purity (HPLC), ^{1}H NMR δ6.90 (1H, s), 6.87–6.81 (1H, q, J = 7.2 Hz), 3.78 (3H, s), 2.15 (3H, s), 1.80–1.78 (3H, d, J = 7.2 Hz); ^{13}C NMR δ168.2 (s), 165.1 (s), 134.3 (s), 125.9 (s), 52.4 (s), 23.5 (s), 14.9 (s). Ac-(*E*)-ΔAbu-OMe: 91% purity (HPLC), ^{1}H NMR δ7.42 (1H, s), 7.21–7.15 (1H, q, J = 7.6 Hz), 3.85 (3H, s), 2.08 (3H, s), 1.79–1.77 (3H, d, J = 7.6 Hz); ^{13}C NMR δ168.8 (s), 165.1 (s), 128.7 (s), 125.6 (s), 52.3 (s), 24.6 (s), 14.4 (s).

Ac-ΔAla-OMe

Ac-ΔAla-OH (0.129 g, 1 mM), KOH (0.056 g, 1 mM), and MeI (0.142 g, 1 mM) were dissolved in MeOH (6 ml). The mixture was vigorously stirred using a magnetic stirrer at room temperature for 72 h. The solvent was evaporated, Et_2O was added (20 ml), and the mixture was filtered. The filtrate was evaporated and the remaining crude product was purified using flash column chromatography using AcOEt/hexane as the eluent. 100% purity (HPLC), ^{1}H NMR δ7.66 (1H, s), 6.54 (1H, s), 5.82 (1H, s), 3.78 (3H, s), 2.07 (3H, s); ^{13}C NMR δ167.8 (s), 163.6 (s), 129.8 (s), 107.7 (s), 52.0 (s), 23.7 (s).

FTIR Spectroscopy

The IR spectra were recorded at 20 °C using a Nicolet 540 Magna spectrometer equipped with DTGS detector and flushed with dry nitrogen during the measurements. All spectra were recorded at 2 cm^{-1} resolution and averaged using 256 scans. Solvent spectra obtained under identical conditions were subtracted from sample spectra. The spectra were analysed with the GRAMS/AI version 9.00 R2 (Thermo Fisher Scientific, Waltham, Massachusetts, USA). The number and position of component bands were obtained by Fourier self-deconvolution techniques and by means of the second derivative as an 'initial guess'. Then the accurate band positions were determined by the curve-fitting procedure with a mixed (Gauss-Lorentz) profile. The thickness of the KBr liquid cell was 0.6 mm. The concentration was varied between 5.8–7.0 × 10^{-3} mol/l.

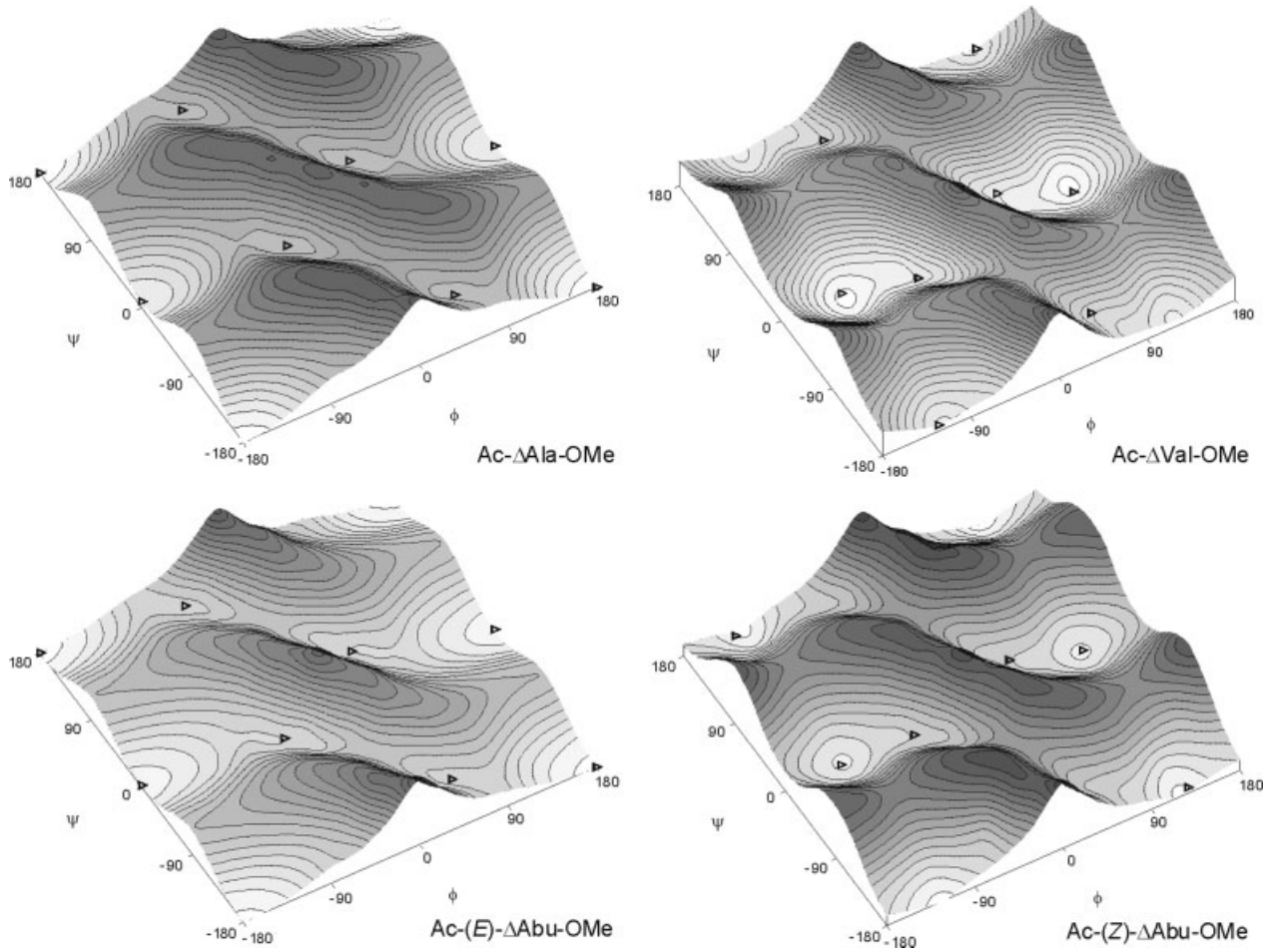

Figure 3. The φ, ψ potential energy surfaces and conformers of the studied molecules calculated *in vacuo*.

Results and Discussion

Theoretical Calculations

The ϕ, ψ potential energy surfaces of the studied molecules showed in Figures 3–5 and their conformers described in Table 1 show that the dehydroamino acid residue with a *C*-terminal ester group is able to adopt four conformations: extended C5, semi-extended $\beta 2$, right-handed helical α, and collagen-like β. Additionally, the lack of asymmetry of the α-carbon atom enables the residue to adopt conformations having opposite signs of the torsion angles but equal in energy, as it is shown on the maps.

The results of the calculations showed in Figure 3 and Table 1 show that *in vacuo* all the studied residues have two low-energy conformations, C5 and $\beta 2$. In the case of ΔAla the conformation C5 is the lowest in energy and $\beta 2$ the second lowest. For both ΔAbu residues the order is the same, however, the gap in energy between these conformations is smaller. For ΔVal the order is reversed, the lowest in energy is the conformation $\beta 2$ and the second is the conformation C5. Both conformations are stabilised primarily by the N–H···O hydrogen bonds and also by the weaker C–H···O interactions (Table 2). It should be noted that for the N–H···O hydrogen bond in the conformation C5, the oxygen atom of the *C*-terminal carbonyl group is the proton acceptor, whereas in the conformation $\beta 2$ the same role is played by the oxygen atom of the alkoxy group. Thus, the strength of these N–H···O hydrogen bonds is different. There is also a difference in the geometry structure of the conformations C5 and $\beta 2$ for ΔAla and (*E*)-ΔAbu and for those for (*Z*)-ΔAbu and ΔVal. For ΔAla and (*E*)-ΔAbu, the conformations C5 and $\beta 2$ are completely planar with the values of the torsion angles ϕ, ψ equal to -180°, 180° and -180°, 0°, respectively. The *N*-terminal amide bond, the $C^\alpha{=}C^\beta$ double bond, and the *C*-terminal ester bond are coplanar. Therefore, a π-electron conjugation expanded over these structural elements must be considered as an important stabilising factor. For (*Z*)-ΔAbu and ΔVal, the values of the torsion angle ϕ deviate from planarity. This is the result of a steric hindrance imposed by the side chain substituent in the position *Z*. In results, the π-electron conjugation can be considered only between the $C^\alpha{=}C^\beta$ double bond and the *C*-terminal ester bond. The parameters of the N–H···O hydrogen bonds are also worsened (Table 2). It can be concluded, therefore, that both the N–H···O hydrogen bond and the π-electron conjugation stabilise more efficiently the conformations C5 and $\beta 2$ for ΔAla and (*E*)-ΔAbu than for (*Z*)-ΔAbu and ΔVal residues. This can be seen in the relative energy differences between the conformations C5 and $\beta 2$ and the conformations α and β, which are stabilised mainly by dipole attraction between carbonyl groups [17]. For ΔAla with no β-substituents at the side chain, the energy difference is the highest. In contrast, it is the lowest for ΔVal with two β-substituents. For ΔAbu residues, the gap in energy has intermediate values, but again, the conformation α is relatively lower in energy for (*Z*)-ΔAbu than for (*E*)-ΔAbu. The conformer β

Journal of PeptideScience

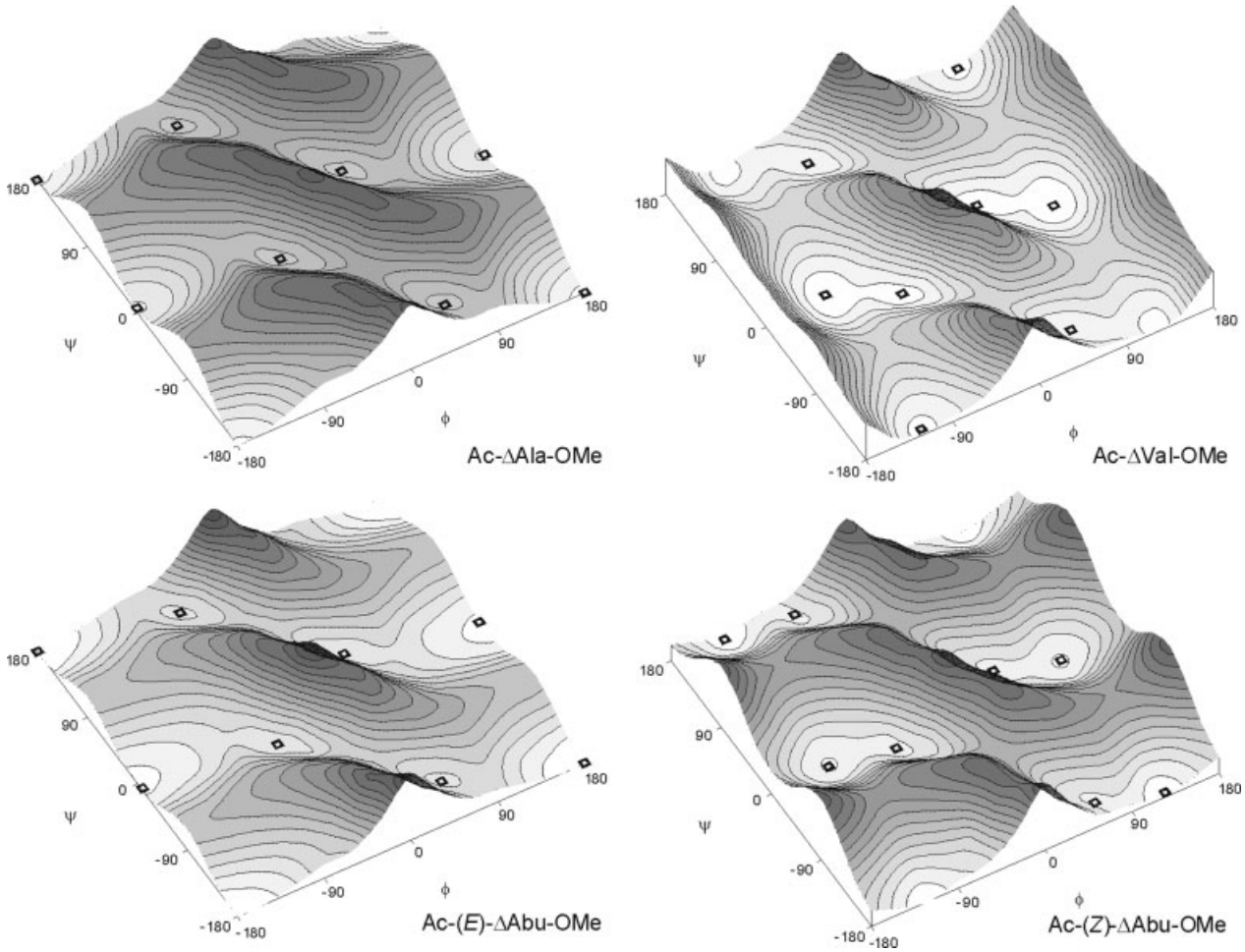

Figure 4. The φ, ψ potential energy surfaces and conformers of the studied molecules calculated in a chloroform-mimicking environment.

was not detected for (*Z*)-ΔAbu *in vacuo* by the theoretical method used. However, it appears in the polar environment.

Figure 4 and Table 1 show the results of the calculations performed in a chloroform-mimicking environment. As can be seen, a weakly polar environment barely changes the energetic order of the conformations for the ΔAla and both ΔAbu residues. The conformations C5 and $\beta 2$ are still the lowest in energy. However, the energy gap between the conformations C5 and $\beta 2$ and the conformations α and β decreases considerably. Again the conformations α and β seem to be much more easily accessible for (*Z*)-ΔAbu than those for (*E*)-ΔAbu. The greatest effect is for the ΔVal residue. The conformation $\beta 2$ is still the most preferred, but the energy of the conformation α is almost equal and the energy differences between the ΔVal conformations do not exceed 0.8 kcal/mol.

In a more polar, water-mimicking environment (Figure 5 and Table 1) greater differences in the conformational preferences of the studied residues are revealed. The properties of the ΔAla residue are similar to those in the gas phase. The conformation C5 is the most favourable and the second is the conformation $\beta 2$. The conformations α and β still remain considerably high in the energy order and seem to be inaccessible. In contrast, the ΔVal residue prefers the conformations α, and β, then the conformations $\beta 2$, whereas the conformation C5 is disfavoured.

For ΔAbu residues, the differences among the conformations' energies are diffused to a value as low as 0.8 kcal/mol for (*E*)-ΔAbu and even 0.3 kcal/mol for (*Z*)-ΔAbu. Thus, all conformations seem to be accessible. Nevertheless, for (*E*)-ΔAbu, the conformation C5 should be preferred, and then the conformations α and $\beta 2$ of almost equal energy, but the conformation β should be disfavoured. For (*Z*)-ΔAbu, the theoretical simulations predict that the conformations α and β are very close in energy order to the lowest conformation C5, but the conformation $\beta 2$ should be rather disfavoured.

Thus, the ΔAbu residues reveal intermediate conformational properties in comparison with those of ΔAla and ΔVal. It should be noted that the properties of the (*E*)-ΔAbu residue are rather close to those of ΔAla, whereas the (*Z*)-ΔAbu residue rather resembles those of ΔVal.

IR analysis

Figure 6 shows the ν_s(N–H)-stretching mode region of the Fourier transform IR (FTIR) spectra of the studied molecules in non-polar CCl_4 and weakly polar $CHCl_3$ solutions. All bands observed in this region were assigned to the NH-stretching vibrations in monomers, except for those absorptions at 3394 and 3386 cm^{-1} in the ΔVal residue spectrum, which are probably due to first overtone of amide I modes.

In the CCl_4 solution, the bands at 3415–3418 cm^{-1} indicate the internal N–H···O hydrogen bond and can be assigned to the conformation C5. The bands are the most intense for the ΔAla

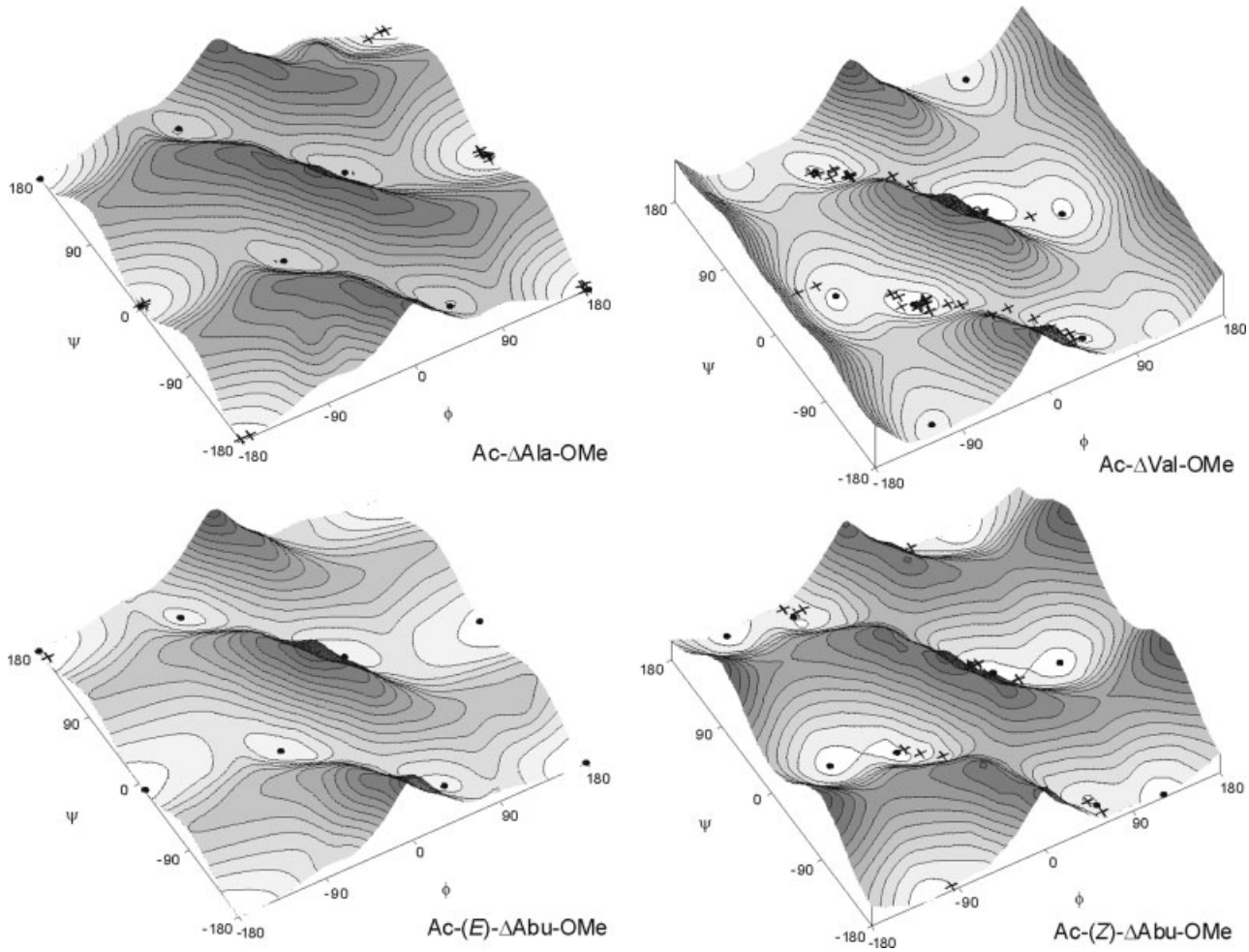

Figure 5. The φ, ψ potential energy surfaces and conformers of the studied molecules calculated in a water-mimicking environment. Crosses depict the conformations found in the solid state (Table 4).

and both ΔAbu residues. It means that for these residues the conformation C5 is preferred. In contrast, for the ΔVal residue the band at 3418 cm^{-1} has relatively low intensity. In the CCl_3 solution, the bands at 3409–3417 cm^{-1} correspond to the conformations C5 of the ΔAla and both ΔAbu residues. The band assigned to conformation C5 is not present for ΔVal residue. The positions of these bands, 3409, 3411, and 3417 cm^{-1}, respectively for ΔAla, (*E*)-ΔAbu, and (*Z*)-ΔAbu indicate the relative strength of the N–H···O hydrogen bonds stabilising the conformations C5. The band of the NH-stretching mode in the spectrum of the saturated analogue Ac-Ala-OMe in CH_2Cl_2 solution occurs at 3432 cm^{-1} [18]. In the case of amides of dehydroamino acids, the bands corresponding to the conformations C5 are observed at 3379–3411 cm^{-1} [19,20]. It can be concluded, therefore, that the C5-type N–H···O hydrogen bond is stronger in dehydroamino acid esters than for saturated analogues but slightly weaker than for dehydroamino acid amides.

The ν_s(N-H) bands at 3438–3455 cm^{-1} in the CCl_4 and at 3430–3445 cm^{-1} in the $CHCl_3$ solutions of the studied molecules indicate that it is not only the conformation C5 which is present in the solutions. Again, some similarities between the (*Z*)-ΔAbu and ΔVal and the ΔAla and (*E*)-ΔAbu residues can be observed. For the ΔVal residue, the bands at 3438 cm^{-1} in CCl_4 and at 3430 cm^{-1} in $CHCl_3$ are relatively narrow ($\Delta\nu_{1/2}$ = 15 and 28 cm^{-1}, respectively). This means that they originate from a single conformation. The position of these bands shows that an N–H amide proton is involved in a hydrogen bond interaction, but weaker in comparison to that in the conformation C5. Therefore, it can be assigned to the conformation $\beta 2$, where the N–H···O hydrogen bond can be created using the oxygen atom of the alcoxy group as a proton acceptor. For the (*Z*)-ΔAbu residue, similar bands are present (3440 cm^{-1} in CCl_4 and 3435 cm^{-1} in $CHCl_3$), although with smaller intensities. These bands can be also assigned to the conformation $\beta 2$.

For both ΔAla and (*E*)-ΔAbu, the position of their second ν_s(N–H) bands (3455 cm^{-1} in CCl_4 and at 3445 cm^{-1} in $CHCl_3$) are the same. The energy orders of the calculated conformers indicate conformation $\beta 2$ as the second choice for both residues. However, the positions of the above mentioned bands are higher than those for (*Z*)-ΔAbu and ΔVal, and are rather typical for free N–H groups. To assign these bands to their proper conformations the theoretical frequencies are shown in Table 3. Interestingly, the values do not differ considerably for the conformations $\beta 2$, α, and β. Nevertheless, the calculated values are closer to the experimental ones when the conformation $\beta 2$ is considered. A possible reason for the high position of the bands for ΔAla and (*E*)-ΔAbu is the flatness of the *N*-terminal part of the molecules in the conformation $\beta 2$. Characteristic for such a conformation is the stabilisation

Table 1. Conformers of the studied Ac-ΔXaa-OMe molecules

Conformer code[a]	ϕ (°)	ψ (°)	Energy (hartrees)	ΔE (kcal/mol)
Ac-ΔAla-OMe				
In vacuo				
C5 βL E	−180.0	180.0	−514.498700	0.00
β2 δL B	−180.0	0.0	−514.495678	1.89
α αL A	−48.5	−28.7	−514.488404	6.46
β εL F	−50.9	152.6	−514.488120	6.64
Chloroform-mimicking environment				
C5 βL E	−180.0	180.0	−514.506405	0.00
β2 δL B	−179.9	0.0	−514.504390	1.27
β εL F	−51.5	151.4	−514.499251	4.49
α αL A	−49.5	−30.7	−514.499155	4.55
Water-mimicking environment				
C5 βL E	−180.0	180.0	−514.509697	0.00
β2 δL B	−179.9	0.0	−514.508312	0.87
β εL F	−52.6	152.0	−514.504522	3.24
α αL A	−50.0	−32.0	−514.504381	3.33
Ac-(Z)-ΔAbu-OMe				
In vacuo				
C5 βL E	−129.4	175.9	−553.795950	0.00
β2 δD B	−125.6	−3.8	−553.794056	1.19
α αL A	−58.0	−16.6	−553.791105	3.04
Chloroform-mimicking environment				
C5 βL E	−126.2	176.5	−553.804189	0.00
β2 δD B	−121.6	−1.8	−553.803280	0.57
α αL A	−60.4	−17.6	−553.802347	1.16
β εL F	−61.5	162.8	−553.802072	1.33
Water-mimicking environment				
C5 βL E	−123.2	178.2	−553.808161	0.00
α αL A	−60.8	−18.9	−553.807801	0.23
β εL F	−62.7	163.4	−553.807717	0.28
β2 αL B	−119.6	−0.9	−553.807618	0.34

Conformer code[a]	ϕ (°)	ψ (°)	Energy (hartrees)	ΔE (kcal/mol)
Ac-(E)-ΔAbu-OMe				
In vacuo				
C5 βL E	−179.9	−179.9	−553.793993	0.00
β2 δL B	−180.0	0.0	−553.792399	1.00
α αL A	−51.2	−28.8	−553.788150	3.67
β εL F	−51.6	145.7	−553.786922	4.44
Chloroform-mimicking environment				
C5 βL E	−179.9	179.4	−553.801634	0.00
β2 δD B	−179.5	−8.6	−553.800499	0.71
α αL A	−52.4	−31.1	−553.798825	1.76
β εL F	−52.1	144.2	−553.798093	2.22
Water-mimicking environment				
C5 βL E	−179.7	179.1	−553.804897	0.00
α αL B	−52.2	−33.6	−553.804211	0.43
β2 δD A	−179.1	−10.1	−553.804169	0.45
β εL F	−53.3	144.4	−553.803598	0.81
Ac-ΔVal-OMe				
In vacuo				
β2 γL B	−118.1	0.3	−593.090513	0.00
C5 βL E	−123.1	−179.9	−593.090100	0.26
α αL A	−54.7	−24.8	−593.088487	1.27
β εL F	−52.8	145.4	−593.087030	2.19
Chloroform-mimicking environment				
β2 γL B	−114.9	6.0	−593.099596	0.00
α αL A	−54.9	−28.3	−593.099488	0.07
C5 εL E	−119.9	−174.7	−593.098651	0.59
β εL F	−53.5	143.4	−593.098391	0.76
Water-mimicking environment				
α αL A	−54.6	−31.0	−593.104966	0.00
β εL F	−54.9	144.3	−593.104127	0.53
β2 γL B	−111.9	9.0	−593.104016	0.60
C5 εL E	−114.3	−167.4	−593.102931	1.28

[a] Each calculated conformer has its mirror counterpart.

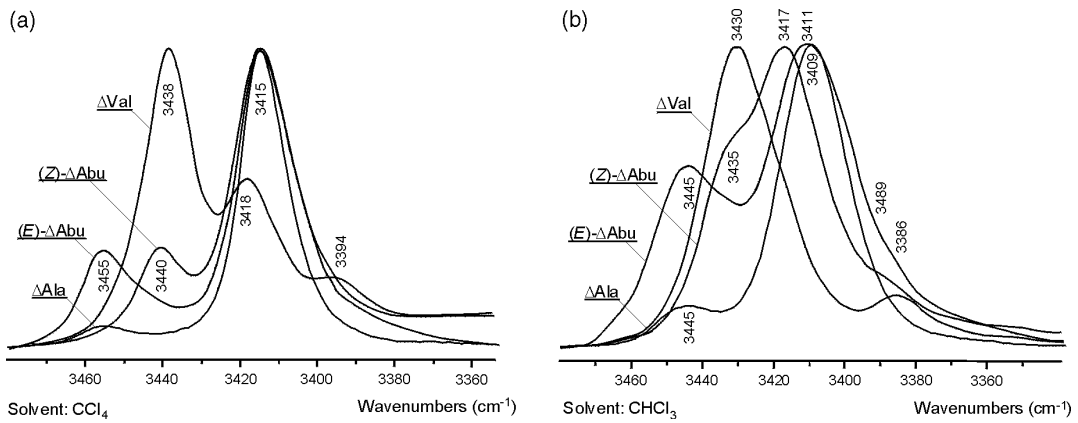

Figure 6. The FTIR spectra of the studied molecules in the ν_s(N-H) region in CCl_4 (a) and $CHCl_3$ (b) solutions.

Table 2. Structural parameters for the internal X–H···A and C=O ▶····◀ C=O interactions in the B3LYP/6–311++G** conformers of the studied molecules in gas phase

Parameters ↓ Conformers →	Ac-ΔAla-OMe				Ac-(*E*)-ΔAbu-OMe				Ac-(*Z*)-ΔAbu-OMe				Ac-ΔVal-OMe			
	C5	β2	α	β	C5	β2	α	β	C5	β2	α	β^c	C5	β2	α	β
N–H···O hydrogen bond[a]																
*r*H···O (Å)	2.15	2.10			2.07	2.06			2.27	2.28			2.23	2.28		
*r*N···O (Å)	2.65	2.60			2.61	2.58			2.69	2.63			2.64	2.64		
∠N–H···O (°)	108.7	108.3			110.9	109.5			103.3	98.6			95.5	102.7		
∠C–O···H (°)	84.9	90.2			86.2	90.4			83.7	88.4			88.0	84.7		
C–H···O hydrogen bond[a]																
*r*H···O (Å)	2.27^{β}	2.26^{β}	2.62^{β}	2.54^{β}	2.13^{β}	2.15^{β}	2.34^{γ}	2.37^{γ}	2.35^{β}	2.45^{β}	2.47^{β}	2.39^{β}	2.50^{γ}	2.55^{γ}	2.27^{γ}	2.32^{γ}
	2.40^{β}	2.48^{β}			2.20^{γ}	2.61^{γ}			2.58^{γ}	2.63^{γ}			2.20^{γ}	2.22^{γ}		
						2.61^{γ}										
*r*C···O (Å)	2.90	2.89	2.89	2.80	2.91	2.91	3.02	3.01	2.77	2.85	2.84	2.77	2.94	2.99	2.92	2.94
	2.76	2.84			2.92	2.82			2.94	2.97			2.83	2.89		
						2.82										
∠C–H···O (°)	115.9	115.8	92.8	92.4	126.9	124.9	118.8	116.1	100.7	100.1	98.5	98.3	102.8	102.8	116.7	113.9
	97.9	97.8			121.8	90.8			97.9	97.5			117.6	114.6		
						90.8										
∠C=O···H (°)	104.7	104.9	77.3	81.9	101.3	102.3	94.9	94.2	86.5	80.3	79.8	85.1	107.1	109.3	94.2	91.3
	87.8	80.9			109.9	99.4			116.5	114.6			99.9	106.9		
						99.4										
C=O ▶····◀ C=O dipole attractions[b]																
$rC^{C}\cdots O^{N}$ (Å)			2.93	2.91			2.95	3.15			3.10	3.16			3.02	2.92
$rC^{N}\cdots O^{C}$ (Å)				3.13				2.90				3.08				3.12
*r*C···C (Å)			3.06	3.00			3.05	2.98			3.12	3.08			3.06	2.96
*r*O···O (Å)			2.94	3.08			3.01	3.16			3.07	3.23			3.78	3.20
$\angle(C{=}O)^{N}\cdots C^{C}$ (°)			84.5	82.6			83.2	81.7			80.0	78.5			80.3	79.8
$\angle O^{N}\cdots(C{=}O)^{C}$ (°)			122.6	86.7			120.0	91.0			128.2	85.9			120.8	91.7
$\angle C^{N}\cdots(O{=}C)^{C}$ (°)			26.9	72.6			28.0	70.8			22.6	74.9			26.8	71.3
$\angle C^{N}\cdots(O{=}C)^{C}$ (°)			64.1	76.3			64.2	79.4			70.0	81.9			67.0	82.5

[a] Data presented only for X–H···A (X=N, C; A=O) in which H···A ≤2.7 Å and ∠X–H···A >90°. $^{\beta}$, $^{\gamma}$ denote C^{β}–H···O and C^{γ}–H···O.
[b] Data presented only for the C=O ▶····◀ C=O contacts, in which C···O ≤3.6 Å according to Ref. 17. ^{N,C} denote the *N*-terminal and *C*-terminal carbonyl group.
[c] Data presented for the conformer β in chloroform.

Table 3. Theoretical amide mode frequencies ν_s(N–H) (per centimetre) of the studied compounds in CCl_4- and $CHCl_3$-mimicking environment calculated at the B3LYP/6–311++G** level

Compound	CCl_4				$CHCl_3$			
	C5	β2	α	β	C5	β2	α	β
Ac-ΔAla-OMe	3408	3448	3450	3454	3406	3442	3447	3450
Ac-(*E*)-ΔAbu-OMe	3406	3453	3455	3456	3404	3448	3452	3453
Ac-(*Z*)-ΔAbu-OMe	3417	3442	3445	–	3423	3440	3444	3444
Ac-ΔVal-OMe	3418	3441	3440	3444	3423	3436	3440	3443

The factor 0.952 was applied to fit the calculated frequencies to the experimental results.

by the C^{β}–H···O=C resonance-assisted intramolecular H-bond closing the six-member flat ring [21,22]. Forming a hydrogen bond by the C=O group, changes the electronic properties of the whole amide moiety and influences the NH proton donor's abilities [23]. This is the reason for the different spectral features of β2 conformations for ΔAla, (*E*)-ΔAbu and (*Z*)-ΔAbu, ΔVal residues.

The results of the IR analysis indicate, again, the same similarities between the (*Z*)-ΔAbu and ΔVal residues as well as ΔAla and (*E*)-ΔAbu ones.

Solid State Conformations

Table 4 shows the solid state conformations of the dehydroamino acid residue with a *C*-terminal ester bond found in the Cambridge Structural Database [24].

As can be seen, the ΔAla residue adopts two conformations C5 and β2 (and their mirror conformations) [25,27,28,30,33]. This indicates that the conformational properties of the ΔAla residue remain almost unchanged regardless of the environment. However, analysis of all the data, theoretical, IR, and solid state,

Journal of PeptideScience

Table 4. Conformations of α,β-dehydroamino acid esters found in the crystal state

Conformation			C^{β}-substituents			Conformation			C^{β}-substituents		
ϕ (°)	ψ (°)	Code	*Z*	*E*	References	ϕ (°)	ψ (°)	Code	*Z*	*E*	References
			Dehydroalanine						*(E)-Dehydrobutyrine analogue*		
−170.33	−178.61	C5	-H	-H	25	−176.63	168.95	C5	-H	-CN	26
176.23	177.75	-C5	-H	-H							
179.60	−173.58	-C5	-H	-H	27				*Dehydrovaline analogues*		
156.20	173.12	-C5	-H	-H	28	53.02	32.32	-α	$-CH_2COOMe$	-Me	29
170.34	178.46	-C5	-H	-H	30	−45.17	−37.76	α	-COOMe	-NHCOPh	31
175.81	−179.87	-C5	-H	-H		45.17	37.76	-α	-COOMe	-NHCOPh	
−179.29	−177.86	C5	-H	-H		33.52	48.66	-α	2-Oxocyclopentylidene		32
176.94	−173.42	-C5	-H	-H	33	−18.15	−106.75	α	$-PO(OEt)_2$	-NHCOPh	34
179.25	−1.38	-β2	-H	-H		−31.13	−52.19	α	-NHCOPh	$-PO(OEt)_2$	
179.25	−1.38	-β2	-H	-H	25	3.57	74.14	-α	-COOMe	-COOMe	35
174.34	3.59	-β2	-H	-H		−23.78	−62.87	α	*Z*-Ile-NH-	-COOMe	36
178.33	0.92	-β2	-H	-H		−65.71	−28.6	α	*Z*-Ile-NH-	-COOMe	
−176.83	−1.54	β2	-H	-H		−45.02	−33.83	α	Boc-NH-	-COOMe	
−179.59	2.37	β2	-H	-H		45.02	33.83	-α	Boc-NH-	-COOMe	
175.93	8.26	-β2	-H	-H		−62.75	−18.65	α	Ph-	-Me	37
−174.89	1.77	β2	-H	-H		−53.04	−37.20	α	Ph-	-Me	
174.69	8.02	-β2	-H	-H		−67.73	−14.00	α	Ph-	-Me	
177.70	−5.88	β2	-H	-H		−50.83	−35.28	α	I-	$-CHMe_2$	38
						−43.51	−32.76	α	Boc-NH-	-COOMe	36
			(Z)-Dehydrobutyrine analogues			−47.65	−47.68	α	Boc-NH-	-COOBzl	
−32.51	−52.29	α	$-NO_2$	-H	39	84.82	0.45	-α	2-(5-Hydroxymethyl)pyrrolidene		40
44.08	31.08	-α	-(R)-3-t-Butoxycarbonyl-2,2-dimethyl-1,3-oxazolidine	-H	41	23.89	−111.56	-β	(EtO)MeCH-	-COOMe	42
−45.11	−33.80	-α	-(R)-3-t-Butoxycarbonyl-2,2-dimethyl-1,3-oxazolidine	-H		−32.72	120.37	β	$-CF_3$	-Ph	43
45.67	34.81	-α	t-Butyl 2-pyrrolidine-1-carboxylate	-H	44	−33.75	118.23	β	$-C(COOMe)(CHNMe_2)$	-COOMe	45
47.98	32.04	-α	$-CH_2CH_2CH(NO_2)Me_2$	-H	46	−34.34	122.59	β	$-C(COOEt)(CHNMe_2)$	$-CF_3$	
52.95	33.85	-α	$-CHMe(NBzl_2)$	-H	47	34.37	−122.57	-β	PHCONH-	-COOMe	36
54.69	19.91	-α	$-CH_2$-(β-Z-(Z)ΔAbu-OMe)	-H	48	39.84	−129.64	-β	Boc-Val-NH-	-COOMe	
−54.69	−19.91	α	$-CH_2$-(β-Z-(Z)ΔAbu-OMe)	-H		46.49	−143.31	-β	*Z*-Pro-NH-	-COOMe	
75.64	0.68	-α	$-NMe_2$	-H	49	−5.97	91.16	β	-COOMe	-NHCOOtBu	50
57.53	−154.71	β	-C≡C-tBu	-H	51	−32.44	122.14	β	-N(Et)(COPh)	-COOMe	
−52.68	164.95	-β	−2S-(Boc-Pro-OEt)	-H	52	−59.41	144.63	β	-Ph	-Me	53
−58.68	165.83	-β	$-CH_2CHPh_2$	-H	54	−54.88	140.26	β	-Me	-Br	55
−58.68	165.83	-β	$-CH_2CHPh_2$	-H	56	47.19	−134.46	-β	-Me	-4-MeOPh	
62.16	−173.41	β	−3-(4,6-Dimethyl-2-pyrimidinylamine	-H	49	6.69	−94.22	-β	-Me	$-NO_2$	39
−66.81	175.35	β	$-CHMe_2$	-H	57	−40.68	135.39	β	-Br	-Ph	58
−97.61	−179.26	β	$-CHMe_2$	-H		−47.42	129.87	β	Boc-NH-	-COOMe	36
67.31	179.05	α_D	$-NHCOCHMe_2$	-H	59	−40.91	137.70	β	Boc-NH-	-COOBzl	
						−121.38	25.80	β2	Boc-NH-	-COOBzl	
						−145.54	19.66	β2	$-SOCH_2$-	-Me	60

shows that an increase in the polarity of the environment promotes the conformation β2.

Unfortunately, for the ΔAbu and ΔVal residues no data is available. Nevertheless, if only the position of the β-substituents is considered, rather than the type, then the analogous structures for ΔAbu and ΔVal residues can be analysed. It has been found that the ΔVal analogues adopt primarily conformations α and β [29,31,32,34–40,42,43,45,50,53,55,58,60]. The conformation β2 can also be found [36,40]. This is consistent with the theoretical calculations performed in a water-mimicking environment for the ΔVal residue. The (*Z*)-ΔAbu analogues also adopt the conformations α and β [41,44,46–49,51,52,54,56,57,59]. Only one (*E*)-ΔAbu analogue was found having a cyanide group in the side chain. It should be noted, however, that

it adopts the conformation C5 [26], similarly to the ΔAla residue.

The distribution of the solid state conformations again shows some similarities between the ΔAla and the dehydroamino acid with the β-substituent in the position *E*, as well as dehydroamino acid residues with the β-substituent in the position *Z*, or both *Z* and *E*.

Conclusions

The α,β-dehydroamino acids with the *C*-terminal ester bond reveal well-defined conformational conservatism. They can only adopt four conformations: extended C5, semi-extended $\beta 2$, helical α, and collagen-like β. The lack of asymmetry of the α-carbon atom makes the mirror conformations, with opposite signs from the torsion angles, equally probable.

The specific conformational feature of the studied α, β-dehydroamino acids is the ability to adopt a semi-extended conformation $\beta 2$. This conformation is not found for saturated depsipeptides [61]. The conformation $\beta 2$ is predicted by theoretical calculations for analogous dehydroamino acid amides but generally it has relatively high energy. Interestingly, although the DFT calculations predict the low-energy conformer $\beta 2$ for the Ac-(*Z*)-ΔAbu-NHMe molecule [62], it is not confirmed by FTIR analysis [20], neither is it adopted in the solid state [62]. Therefore, the low-energy conformation $\beta 2$ is the result of the non-additive junction of both the $C^{\alpha}{=}C^{\beta}$ double bond and ester group within the amino acid residue.

The β-substituents at the side chain have considerable impact on the conformational preferences. The ΔAla residue adopts solely the conformations C5 and $\beta 2$, regardless of the environment. In contrast, the ΔVal residue strongly prefers the conformation $\beta 2$ in a low polar environment, but an increase in the environment polarity promotes the conformations α and β.

The ΔAbu residues reveal intermediate preferences. In an environment with low polarity, both (*E*)-ΔAbu and (*Z*)-ΔAbu prefer first the conformation C5, and then, the conformation $\beta 2$, as in the case of the ΔAla residue. However, in an environment of higher polarity, the (*Z*)-ΔAbu residue tends to adopt the conformations α and β, similar to the ΔVal residue. This is not the case for (*E*)-ΔAbu, which has the properties similar to the ΔAla analogue, and prefers instead the conformations C5 and $\beta 2$.

These studies also show that the ΔAbu and ΔVal residues constitute a basic conformational pattern for all dehydroamino acids with a *C*-terminal ester bond which have the various β-substituents in the positions *Z* or *E*, or both.

The results indicate that a relatively small change of the structure, like the position of the methyl group, can have considerable influence on the conformation of the α,β-dehydroamino acid residue. The change of the geometrical isomers *Z*/*E*, easily obtained in nature, gives an access to diverse conformational feature. Probably, this could be a reason of the presence of dehydrobutyrine in the structures of phomalide and isophomalide.

Acknowledgements

The authors gratefully acknowledge the Academic Computer Centre CYFRONET AGH of Kraków for the grant MniSW/SGI3700/Uopolski/103/2008. Justyna Grondys is a recipient of a PhD fellowship from a project funded by the European Social Fund.

References

1 Bagley MC, Dale JW, Merritt EA, Xiong X. Thiopeptide antibiotics. *Chem. Rev.* 2005; **105**: 685–714.
2 Yoshinari T, Okada H, Yamada A, Uemura D, Oka H, Suda H, Okura A. Inhibition of topoisomerase II by a novel antitumor cyclic depsipeptide, BE-22179. *Jpn. J. Cancer Res.* 1994; **85**: 550–555.
3 Teshima T, Nishikava M, Kubota I, Shiba T, Iwa Y, Omura S. The structure of an antibiotic, dityromycin. *Tetrahedron Lett.* 1988; **29**: 1963–1966.
4 Leibold T, Sassa F, Reichenbach H, Höfle G. Cyrmenins, novel antifungal peptides containing a nitrogen-linked β-methoxyacrylate pharmacophore: isolation and structural elucidation. *Eur. J. Org. Chem.* 2004; **2**: 431–435.
5 Williams RH, Fitt BDL. Differentiating α and β groups of *Leptosphaeria maculans*, causal agent of stem canker (blackleg) of oilseed rape. *Plant Pathol.* 1999; **48**(2): 161–175.
6 Howlett BJ, Idnurm A, Pedras MSC. *Leptosphaeria maculans*, the causal agent of blackleg disease of Brassicas. *Fungal Genet. Biol.* 2001; **33**: 1–14.
7 Pedras MSC, Biesenthal CJ. Vital staining of plant cell suspension cultures: evaluation of the phytotoxic activity of the phytotoxins phomalide and destruxin B. *Plant Cell Rep.* 2000; **19**: 1135–1138.
8 Pedras MSC, Chumala PB, Yu Y. The phytopathogenic fungi *Leptosphaeria maculans* and *Leptosphaeria biglobosa*: chemotaxonomical characterisation of isolates and metabolite production in different culture media. *Can. J. Microbiol.* 2007; **53**: 364–371.
9 Ward DE, Vazquez A, Soledade M, Pedras C. Phytotoxicity: synthesis and biological discrimination of phomalide and its (*Z*)-isomer. *J. Org. Chem.* 1996; **61**: 8008–8009.
10 Ward DE, Vázquez A, Pedras MSC. Probing host-selective phytotoxicity: synthesis and biological activity of phomalide, isophomalide, and dihydrophomalide. *J. Org. Chem.* 1999; **64**: 1657–1666.
11 Frisch MJ, Trucks GW, Schlegel HB, Scuseria GE, Robb MA, Cheeseman JR, Scalmani G, Barone V, Mennucci B, Petersson GA, Nakatsuji H, Caricato M, Li X, Hratchian HP, Izmaylov AF, Bloino J, Zheng G, Sonnenberg JL, Hada M, Ehara M, Toyota K, Fukuda R, Hasegawa J, Ishida M, Nakajima T, Honda Y, Kitao O, Nakai H, Vreven T, Montgomery JA, Jr, Peralta JE, Ogliaro F, Bearpark M, Heyd JJ, Brothers E, Kudin KN, Staroverov VN, Kobayashi R, Normand J, Raghavachari K, Rendell A, Burant JC, Iyengar SS, Tomasi J, Cossi M, Rega N, Millam JM, Klene M, Knox JE, Cross JB, Bakken V, Adamo C, Jaramillo J, Gomperts R, Stratmann RE, Yazyev O, Austin AJ, Cammi R, Pomelli C, Ochterski JW, Martin RL, Morokuma K, Zakrzewski VG, Voth GA, Salvador P, Dannenberg JJ, Dapprich S, Daniels AD, Farkas O, Foresman JB, Ortiz JV, Cioslowski J, Fox DJ. *Gaussian 09, Revision A.1*. Gaussian Inc.: Wallingford CT, 2009.
12 Tomasi J, Mennucci B, Cammi R. Quantum mechanical continuum salvation models. *Chem. Rev.* 2005; **105**: 2999–3093.
13 Miertus S, Tomasi J. Approximateevaluationsof theelectrostatic free energy and internal energy changes in solution processes. *Chem. Phys.* 1982; **65**: 239–245.
14 Hudáky I, Kiss R, Perczel A. A nomenclature of peptide conformers. *J. Mol. Struct. (Theochem)* 2004; **675**: 177–183.
15 Schöllkopf U, Meyer R. *N*-acyldehydro-α-aminosäuren aus *N*-formyldehydro-α-aminosäure-methylestern. *Liebigs Ann. Chem.* 1981; 1469–147.
16 Wieland T, Ohnacker G, Ziegler W. Aminosaure-synthesen mit alpha-acylamino-acrylestern. *Chem. Ber.* 1957; **90**: 194–201.
17 Allen FH, Baalham CA, Lommerse JPM, Raithby PR. Carbonyl-carbonyl interactions can be competitive with hydrogen bonds. *Acta Crystallogr. B* 1998; **54**: 320–329.
18 Gallo EA, Gellman SH. Hydrogen-bond-mediated folding in depsipeptide models of β-turns and α-helical turns. *J. Am. Chem. Soc.* 1993; **115**: 9774–9788.
19 Broda MA, Rzeszotarska B, Smełka L, Rospenk M. Conformational investigation of α,β-dehydropeptides. VIII. *N*-acetyl-α, β-dehydroamino acid *N*′-methylamides: conformation and electron density perturbation from infrared and theoretical studies. *J. Pept. Res.* 1997; **50**: 342–351.
20 Broda MA, Rzeszotarska B, Smełka L, Pietrzyński G. Conformational investigation of α,β-dehydropeptides. IX. *N*-acetyl-(*E*)-α,β-dehy-

drobutyrine *N*′-methylamide: stereoelectronic properties from infrared and theoretical studies. *J. Pept. Res.* 1998; **52**: 72–79.
21 Sobczyk L, Grabowski SJ, Krygowski TM. Interrelation between H-bond and Pi-electron delocalization. *Chem. Rev.* 2005; **105**: 3513–3560.
22 Crisma M, Formaggio F, Toniolo C, Yoshikawa T, Wakamiya T. Flat peptides. *J. Am. Chem. Soc.* 1999; **121**: 3272–3278.
23 Herrebout W, Clou K, Desseyn HO, Blaton N. Vibrational characterization of the peptide bond. *Spectrochimica Acta A* 2003; **59**: 47–59.
24 Allen FH. The cambridge structural database: a quarter of a million crystal structures and rising. *Acta Crystallogr. B* 2002; **58**: 380–388. (http://www.ccdc.cam.ac.uk/).
25 Dey S, Vijayaraghavan R, Goel VK, Kumar S, Kumar P, Singh TP. Design rules for peptides with α, β-dehydro-residues: synthesis of a model peptide Boc-Ile-δAla-OCH3 and its crystal structures obtained from two different solvents. *J. Mol. Struct.* 2005; **737**(2–3): 109–116.
26 GolobiŠ A, Koller J. Conformational analysis of 2,3-substituted propenoates. *J. Mol. Struct. (THEOCHEM)* 2002; **532**: 109–126.
27 Piazzesi AM, Bardi R, Crisma M, Toniolo C, Singh M, Chauhan VS. Molecular and crystal structure of a dehydroalanine dipeptide. *Z. Kristallogr.* 1993; **207**: 25–32.
28 Padmanabhan B, Dey S, Khandelwal B, Subba Rao G, Singh TP. Design of peptides: synthesis, crystal structure, molecular conformation, and conformational calculations of N-Boc-L-Phe-dehydro-Ala-OCH_3. *Biopolymers* 1992; **32**(10): 1271–1276.
29 Mapelli C, Elrod LF, Holt EM, Stammer CH. The synthesis and characterization of 2,3-methanopyroglutamic acid. *Tetrahedron* 1989; **45**(14): 4377–4382.
30 Crisma M, Formaggio F, Toniolo C, Yoshikawa T, Wakamiya T. Flat peptides. *J. Am. Chem. Soc.* 1999; **121**(14): 3272–3278.
31 Schumann S, Steglich W, Polborn K. *Private communication to the Cambridge Structural Database*, 2004; deposition number CCDC 258144.
32 Schwarz T, Steglich W, Polborn K. *Private communication to the Cambridge Structural Database*, 2004; deposition number CCDC 258148.
33 Pinheiro AC, Kaiser CR, Lourenço MCS, De Souza MVN, Wardell SMSV, Wardell JL. Synthesis and in vitro activity towards Mycobacterium tuberculosis of L-serinyl ester and amino derivatives of pyrazinoic acid. *J. Chem. Res.* 2007; **3**: 180–184.
34 Haug C, Steglich W, Polborn K. *Private communication to the Cambridge Structural Database*, 2004; deposition number CCDC 255310.
35 Busetti V, Ajo D, De Zuane F. Crystal state conformation of a β,β'-disubstituted dehydroaminoacid derivative. *Z. Kristallogr.* 1988; **184**(3–4): 203–208.
36 Schumann S, Steglich W, Polborn K. *Private communication to the Cambridge Structural Database*, 2005; deposition numbers CCDC 265787, 266628, 265915, 266004, 263359, 263479.
37 Parsons S, Bell S, Turner NJ, Johnstone R. *Private communication to the Cambridge Structural Database*, 2006; deposition number CCDC 611728.
38 Michaux J, Retailleau P, Campagne J-M. Synthesis of the central tryptophan-leucine residue of celogentin C. *Synlett* 2008; **10**: 1532–1536.
39 Easton CJ, Roselt PD, Tiekink ERT. Crystal structure of methyl (Z)-2-benzamido-3-nitroprop-2-enoate, $C_{11}H_{10}N_2O_5$. *Z. Kristallogr.* 1996; **211**: 195.
40 Landreau CAS, LePla RC, Shipman M, Slawin AMZ, Hartley JA. Delineating noncovalent interactions between the azinomycins and double-stranded DNA: importance of the naphthalene substitution pattern on interstrand cross-linking efficiency. *Org. Lett.* 2004; **6**(20): 3505–3507.
41 Avenoza A, Cativiela C, Peregrina JM, Zurbano MM. Synthesis of meso-2,4-diaminoglutaric acid. *Tetrahedron: Asymm.* 1996; **7**(6): 1555–1558.
42 De Risi C, Pollini GP, Veronese AC, Bertolasi V. A new simple route for the synthesis of (±)-2-azetidinones starting from β-enaminoketoesters. *Tetrahedron* 2001; **57**(51): 10155–10161.
43 Enders D, Chen Z-X, Raabe G. Stereoselective synthesis of 3-substituted ethyl (Z)-4,4,4-trifluoro-2- formylamino-2-butenoates. *Synthesis* 2005; **2**: 306–310.
44 Vaswani RG, Chamberlin AR. Stereocontrolled total synthesis of (−)-kaitocephalin. *J. Org. Chem.* 2008; **73**(5): 1661–1681.
45 UršiŠ U, Grošelj U, Meden A, Svete J, Stanovnik B. Regiospecific [2 + 2] cycloadditions of electron-poor acetylenes to (Z)-2-acylamino-3-dimethylaminopropenoates: synthesis of highly functionalised buta-1,3-dienes. *Tetrahedron Lett.* 2008; **49**(23): 3775–3778.
46 Singh J, Kronenthal DR, Schwinden M, Godfrey JD, Fox R, Vawter EJ, Zhang B, Kissick TP, Patel B, Mneimne O, Humora M, Papaioannou CG, Szymanski W, Wong MKY, Chen CK, Heikes JE, DiMarco JD, Qiu J, Deshpande RP, Gougoutas JZ, Mueller RH. Efficient asymmetric synthesis of the vasopeptidase inhibitor BMS-189921. *Org. Lett.* 2003; **5**(17): 3155–3158.
47 Reetz MT, Kayser F, Harms K. Cycloaddition reactions of γ-amino α,β-didehydro amino acid esters: a test case for the principle of 1,3-allylic strain. *Tetrahedron Lett.* 1992; **33**: 3453–3456.
48 Klepp KO, Hiebl J, Kollmann H, Rovenszky F. The crystal structure of dimethyl (2Z, 6Z)-2,7-bis-(benzyloxycarbonylamino)octa-2,6-diendioate: A useful precursor for optically pure 2,7-diaminosuberic acid. *Z. Naturforsch. B: Chem. Sci.* 1999; **54**(4): 447–450.
49 Djinovic-Carugo K, Golic L, Leban I, Svete J, Stanovnik B, Tisler M, Tate C. Three substituted 3-amino-2-benzoylaminopropenoic acid derivatives. *Acta Crystallogr. C: Cryst. Struct. Commun.* 1994; **50**: 239–245.
50 Zeitler K, Steglich W, Polborn K. *Private communication to the Cambridge Structural Database*, 2005; deposition numbers CCDC 267220, 267595.
51 Canisius J, Schurmann M, Preut H, Krause N. Crystal structure of ethyl (Z)-2-(acetylamino)-6,6-dimethyl-2-hepten-4-ynoate, $C_{13}H_{19}NO_3$. *Z. Kristallogr. New Crystal. Struct.* 2001; **216**: 599–600.
52 Mulzer J, Schulzchen F, Bats J-W. Rigid dipeptide mimetics. Stereocontrolled synthesis of all eight stereoisomers of 2-oxo-3-(N-Cbz-amino)-1-azabicyclo[4.3.0]nonane-9-carboxylic Acid ester. *Tetrahedron* 2000; **56**(25): 4289–4298.
53 Parsons S, Eve T, Turner NJ, Johnstone R. *Private communication to the Cambridge Structural Database*, 2006; deposition number CCDC 611747.
54 Groundwater PW, Sharif T, Arany A, Hibbs DE, Hursthouse MB, Nyerges M. Tetrahedron Lett. A new synthesis of didehydroamino acid esters. *Tetrahedron Lett.* 1998; **39**(11): 1433–1436.
55 Parsons S, Roff G, Turner NJ, Johnstone R, Johnstone R. *Private communication to the Cambridge Structural Database*, 2006; deposition numbers CCDC 611749, 611750.
56 Groundwater PW, Sharif T, Arany A, Hibbs DE, Hursthouse MB, Nyerges M. A novel synthesis of didehydroamino acid esters from azomethine ylides. *J. Chem. Soc., Perkin Trans.* 1998; **1**(17): 2837–2846.
57 Narula P, Patel HC, Singh TP. Crystal structure and molecular conformation of N-Boc-L-Pro-dehydro-Leu-OCH_3. *Biopolymers Pept. Sci. Sect.* 1988; **27**(10): 1595–1606.
58 Jones PG, Jäger S. Ethyl (Z)-3-bromo-2-[(tert-butoxycarbonyl)-amino]-3-phenylacrylate. *Acta Crystallogr. E: Struct. Rep. Online* 2003; **59**(3): 369–371.
59 Gunda TE. Rearrangement and degradation of cephalosporins and penicillins in the presence of mercury(II) trifluoroacetate. *Org. Lett.* 2000; **2**: 103–105.
60 Crescenza A, Botta M, Corelli F, Santini A, Tafi A. Cyclic dipeptides. 3.1 Synthesis of methyl (R)-6-[(tert-butoxycarbonyl)amino]-4,5,6,7-tetrahydro-2-methyl-5-oxo-1,4-thiazepine-3-carboxylate and its hexahydro analogues: elaboration of a novel dual ACE/NEP inhibitor. *J. Org. Chem.* 1999; **64**(9): 3019–3025.
61 Siodłak D, Janicki A. Conformational properties of the residues connected by ester and methylated amide bonds. Theoretical and solid state conformational studies. *J. Pept. Sci.* 2010; **16**: 126–135.
62 Siodłak D, Grondys J, Lis T, Bujak M, Broda MA, Rzeszotarska B. The conformational properties of dehydrobutyrine and dehydrovaline: theoretical and solid state conformational studies. *J. Pept. Sci.* 2010; **16**: 496–505.

